Mutation of Serine 395 of Tyrosine Hydroxylase Decouples Oxygen−Oxygen Bond Cleavage and Tyrosine Hydroxylation†

Holly R. Ellis,‡ S. Colette Daubner,‡ and Paul F. Fitzpatrick*,‡,§

Department of Biochemistry and Biophysics and Department of Chemistry, Texas A&M University, College Station, Texas 77843-2128

Received December 13, 1999; Revised Manuscript Received February 8, 2000

ABSTRACT: Ser395 and Ser396 in the active site of rat tyrosine hydroxylase are conserved in all three members of the family of pterin-dependent hydroxylases, phenylalanine hydroxylase, tyrosine hydroxylase, and tryptophan hydroxylase. Ser395 is appropriately positioned to form a hydrogen bond to the imidazole nitrogen of His331, an axial ligand to the active site iron, while Ser396 is located on the wall of the active site cleft. Site-directed mutagenesis has been used to analyze the roles of these two residues in catalysis. The specific activities for formation of dihydroxyphenylalanine by the S395A, S395T, and S396A enzymes are 1.3, 26, and 69% of the wild-type values, respectively. Both the S395A and S396A enzymes bind a stoichiometric amount of iron and exhibit wild-type spectra when complexed with dopamine. The K_M values for tyrosine, 6-methyltetrahydropterin, and tetrahydrobiopterin are unaffected by replacement of either residue with alanine. Although the V_{max} value for tyrosine hydroxylation by the S395A enzyme is decreased by 2 orders of magnitude, the V_{max} value for tetrahydropterin oxidation by either the S395A or the S396A enzyme is unchanged from the wild-type value. With both mutant enzymes, there is quantitative formation of 4a-hydroxypterin from 6-methyltetrahydropterin. These results establish that Ser395 is required for amino acid hydroxylation but not for cleavage of the oxygen−oxygen bond, while Ser396 is not essential. These results also establish that cleavage of the oxygen−oxygen bond occurs in a separate step from amino acid hydroxylation.

Tyrosine hydroxylase (TyrH)[1] belongs to a family of closely related pterin-dependent monooxygenases that includes phenylalanine hydroxylase and tryptophan hydroxylase. All three proteins catalyze the hydroxylation of an aromatic amino acid, utilizing tetrahydrobiopterin (BH_4), oxygen, and a non-heme iron atom (*1*−*3*). Tyrosine hydroxylase catalyzes the formation of dihydroxyphenylalanine (DOPA), the rate-limiting step in the biosynthesis of catecholamine neurotransmitters, with a 4a-hydroxytetrahydropterin as the other product (Scheme 1). Phenylalanine hydroxylase and tryptophan hydroxylase are also rate-limiting enzymes in critical metabolic pathways, catalyzing the hydroxylation of phenylalanine to tyrosine and tryptophan to 5-hydroxytryptophan, respectively. These enzymes are homologous in their C-terminal catalytic domains, but the N-terminal regulatory domains are distinct.

The three-dimensional structure of the catalytic domain of rat TyrH has recently been determined (*4*). The active site is composed of a cleft of four helices made up of mostly hydrophobic residues. The iron atom, located 10 Å from the surface within this cleft, is coordinated by His331, His336, and Glu376. This structure has allowed the identification of active site residues in tyrosine hydroxylase which are conserved across this family of enzymes (Figure 1). We have previously used site-directed mutagenesis to evaluate the roles of several of these residues, including Phe300, Phe309, Arg316, Glu326, Asp328, Glu332, and Tyr371 (*5*−*7*). Two conserved active site residues which have not been analyzed yet are Ser395 and Ser396. The hydroxyl group of Ser395 is within hydrogen bonding distance (2.78 Å) of the N-1 position of the imidazole ring of His331, suggesting that it may play a role in stabilization of the iron center. While Ser396 is also a conserved active site residue, located on the wall of the active site cleft, its role is not apparent from the three-dimensional structure. The results reported herein describe the results of replacement of Ser395 and Ser396 with alanine.

Scheme 1

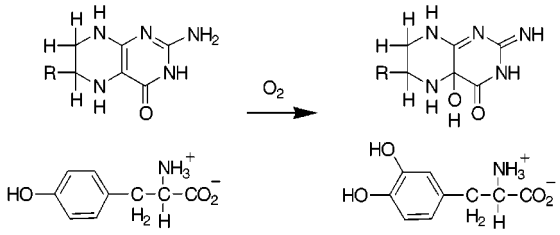

† This research was supported in part by NIH Grant GM R01 47291 and Robert A. Welch Foundation Grant A-1245 to P.F.F. and NIH Grant GM F32 20116 to H.R.E.

* To whom correspondence should be addressed: Department of Biochemistry and Biophysics, Texas A&M University, College Station, TX 77843-2128. Phone: (979) 845-5487. Fax: (979) 845-4946. E-mail: fitzpat@tamu.edu.

‡ Department of Biochemistry and Biophysics.

§ Department of Chemistry.

[1] Abbreviations: DOPA, dihydroxyphenylalanine; TyrH, tyrosine hydroxylase; BH_4, tetrahydrobiopterin; 6-MPH_4, 6-methyltetrahydropterin; K_{tyr}, K_M value for tyrosine; K_{6-MPH4}, K_M value for 6-methyltetrahydropterin; K_{BH4}, K_M value for tetrahydrobiopterin.

10.1021/bi9928546 CCC: $19.00
Published on Web 03/16/2000

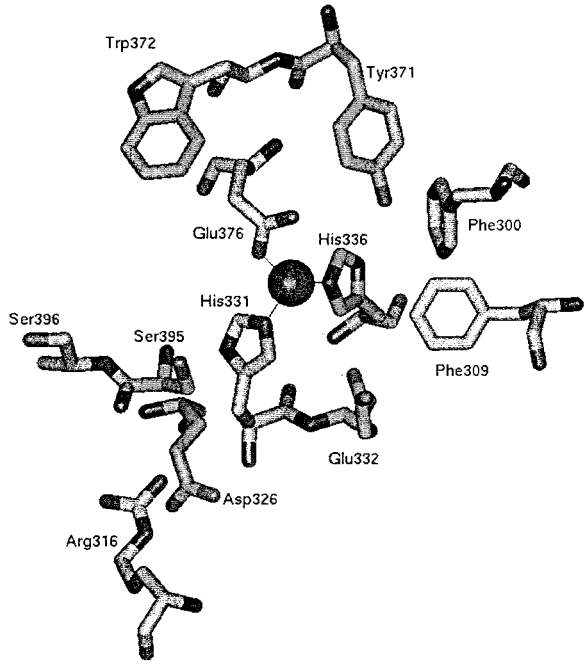

FIGURE 1: Conserved residues in the active site of TyrH. The figure was constructed using PDB file 1TOH.

EXPERIMENTAL PROCEDURES

Materials. Oligonucleotides were synthesized on an Applied Biosystems model 380B DNA synthesizer by the Gene Technology Laboratory of Texas A&M University. Restriction endonucleases *Hin*cII, *Bst*UI, and *Nhe*I were from New England Biolabs Inc. *Pfu* DNA polymerase was obtained from Stratagene USA. Plasmids were purified using kits from Qiagen Inc. DNA sequencing was done by the Gene Technology Laboratory of Texas A&M University. (6*R*)-BH_4 was from Calbiochem. 6-Methyltetrahydropterin (6-MPH_4) was purchased from B. Schircks Laboratories. Leupeptin, pepstatin, and catalase were obtained from Boehringer Mannheim Corp. Sheep dihydropteridine reductase, L-tyrosine, and NADH were from Sigma Corp. Heparin−Sepharose was purchased from Pharmacia Biotech Inc.

Vectors for Enzyme Expression. The Stratagene QuikChange kit was used to replace Ser395 with alanine or threonine using the oligonucleotides 5′-CTCCGTAGGAAGCTAG-CAGCCCTGCAC-3′ and 5′-GCAGGGTGTTGACGTC-CTACGGAGAGC-3′, respectively, and to replace Ser396 with alanine using the oligonucleotide 5′-AGGGCTGCT-GTCCGCGTACGGAGAGCT-3′. Plasmid pETYH8 has been previously described and was used as the template for mutagenesis (*8*). Mutated plasmids were detected by electrophoretic analysis of restriction digests of plasmids, using *Nhe*I for S395A, *Hin*cII for S395T, and *Bst*UI for S396A. The entire coding regions were sequenced to confirm the desired mutations and to detect unexpected mutations. The correct plasmids were named pETYHS395A, pETYHS395T, and pETYHS396A, respectively.

Bacterial Cell Growth and Protein Purification. Bacterial cells expressing wild-type rat TyrH were grown as previously described (*5*). To obtain the mutant proteins, plasmids pETYHS396A, pETYHS395T, and pETYHS395A were introduced into competent *Escherichia coli* BL21(DE3) cells. Small cultures of each were stored as 15% glycerol permanent stocks at −80 °C. Cells from permanent stocks containing the appropriate plasmid were plated on LB agar plates containing 100 μg/mL ampicillin; a single colony from such a plate was used to inoculate a 40 mL liquid culture. After incubation of the latter for 5 h at 37 °C, 10−20 mL was used to inoculate each of two 1 L cultures of LB broth containing 100 μg/mL ampicillin. These were maintained at 37 °C until the A_{600} value reached 0.5, after which the flasks were moved to a 22 °C incubator. When the A_{600} value reached 0.8, isopropyl β-D-thioglucanopyranoside was added to a final concentration of 0.4 mM. After 12 h, cells were harvested by centrifugation at 5000*g* for 30 min and stored at −70 °C overnight.

The purifications of the mutant and wild-type proteins were performed as previously described for the wild-type enzyme (*9*) with the following modifications. Nucleic acids were precipitated with 2.5% streptomycin sulfate (w/v). The enzyme was eluted from the heparin−Sepharose column by a linear gradient from 100 to 600 mM potassium chloride (400 mL total volume) in 50 mM HEPES, 10% glycerol, 75 μM diethylenetriaminopentaacetate, 1 μM pepstatin, and 1 μM leupeptin (pH 7.0). Following precipitation of the purified enzyme with 50% ammonium sulfate, the pellet was resuspended in 50 mM HEPES, 10% glycerol, and 150 mM KCl (pH 7.0). Ferrous ammonium sulfate was added to give an iron:subunit ratio of 1.5:1. The enzyme was then dialyzed extensively against the same buffer lacking ferrous ammonium sulfate.

Assays. All kinetic assays and spectral analyses were performed on a Hewlett-Packard 8452 diode array spectrophotometer. Circular dichroism spectroscopy of wild-type and mutant proteins was performed on an Aviv 62DS circular dichroism spectropolarimeter. The iron content of the enzyme was determined as previously described on a Perkin-Elmer model 2380 atomic absorption spectrophotometer equipped with a graphite furnace (*10*).

The specific activity for the formation of DOPA was measured with a colorimetric end-point assay which determines the amount of DOPA that is formed (*8*). Standard conditions for the assay were 0.5 μM TyrH, 50 mM HEPES/NaOH, 100 μg/mL catalase, 10 μM ferrous ammonium sulfate, 250 μM tyrosine, 300 μM 6-MPH_4, pH 7.0, and 32 °C. Assays were carried out for 2 min.

Rates of tetrahydropterin oxidation were determined by measuring the rate of dihydropterin production using a coupled assay with dihydropteridine reductase, monitoring the decrease in absorbance at 340 nm due to NADH oxidation (*11*). The conditions were 0.4 μM TyrH, 50 mM HEPES/NaOH, 50 μg/mL catalase, 200 μM NADH, 10 μM ferrous ammonium sulfate, 0.2 unit/mL sheep dihydropteridine reductase, pH 7.0, and 25 °C. For the determination of steady-state kinetic parameters, the concentration of 6-MPH_4 or BH_4 was varied from 10 to 400 μM with the tyrosine concentration kept constant at 150 μM, or the concentration of tyrosine was varied from 10 to 200 μM with 200 μM 6-MPH_4. The background rate due to autoxidation of the pterin was taken into account when calculating the rate of dihydropterin production. The steady-state kinetic data were fit directly to the Michaelis−Menten equation using the program Kaleidagraph.

To determine the stoichiometry of the amount of amino acid hydroxylated relative to tetrahydropterin oxidized, the rates of dihydropterin formation and production of DOPA

Scheme 2

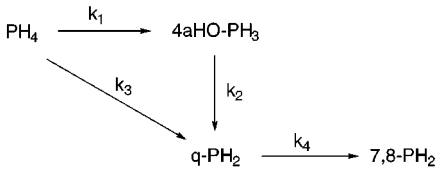

were determined separately on identical samples containing 200 μM 6-MPH$_4$, 150 μM tyrosine, and 0.4 μM TyrH in 50 mM HEPES/NaOH at pH 7.0 and 25 °C. HPLC analyses of the pterin products were performed with 10 μM TyrH, 150 μM tyrosine, 100 μM 6-MPH$_4$, and 10 μM ferrous ammonium sulfate in 20 mM Tris-acetate at pH 8.0 and 25 °C. Twenty seconds after the reaction was initiated by the addition of 6-MPH$_4$, a 20 μL sample was injected onto a Waters HPLC system equipped with a Nova-Pak 3.9 mm × 75 mm C18 column. The products were eluted with an isocratic gradient of 20 mM Tris-acetate (pH 8.0) over the course of 5 min. The elution was monitored at 246 and 300 nm with a Waters model 996 photodiode array detector. The identities of individual peaks were confirmed by using the diode array detector to obtain their absorbance spectra while chromatography experiments were being carried out. The proportions of 4a-hydroxypterin and quinonoid dihydropterin formed enzymatically were determined by following spectrophotometrically the consumption of 100 μM 6-MPH$_4$ by 10 μM TyrH in 50 mM HEPES, 150 μM tyrosine, and 10 μM ferrous ammonium sulfate at pH 8.0 and 25 °C. Spectra were taken from 235 to 500 nm at 2 s intervals for a total of 200 s. The spectra were then analyzed globally using the program SPECFIT (*12*) from Spectrum Software Associates (Chapel Hill, NC) and the mechanism of Scheme 2 to show the contribution of each pterin species as a function of time.

RESULTS

Biophysical Characterization of S395A and S396A TyrH. Ser395 and Ser396, two conserved residues in the active site of TyrH, were replaced with alanine to determine their roles in catalysis. The substitution of serine with alanine is generally considered a conservative substitution, and therefore should not result in any major structural changes. Circular dichroic spectra of the mutant proteins were determined to verify that no major gross changes in secondary structure had occurred as a result of the substitutions. As shown in Figure 2, the spectra for S395A and S396A TyrH are identical to that of the wild-type enzyme.

Even in the absence of gross structural changes, loss of a hydrogen bond between S395A and His331 could lead to disruption of iron binding, resulting in low levels of iron bound to the enzyme. The wild-type enzyme as purified typically contains 0.3−0.6 atom of iron/monomer, but the addition of ferrous ammonium sulfate at the end of the purification increases this value to 0.8−1.0. Atomic absorption spectroscopy was performed to determine the iron content of the mutant and wild-type proteins after such treatment. The stoichiometries were 0.85, 0.90, and 0.92 for S395A, S396A, and wild-type TyrH, respectively.

Purified wild-type TyrH is in the ferric state when isolated and must be subsequently reduced by tetrahydropterin to the active ferrous iron (*10*). Although the active ferrous form of the enzyme is EPR silent, the ferric form is EPR active at

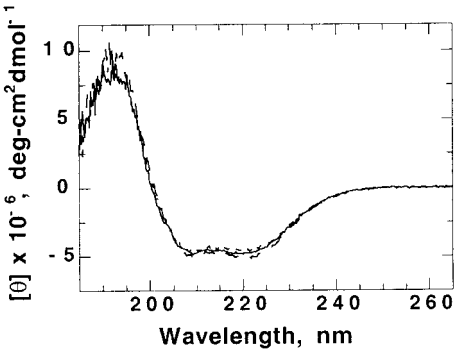

FIGURE 2: Circular dichroic spectra of mutant and wild-type TyrH. Measurements were taken in 0.25 nm increments in a 0.1 cm path length cuvette from 185 to 260 nm with the concentration of protein being 0.2 mg/mL. Each spectrum is the average of three scans. The spectra are for wild-type (solid line), S395A (long-dash line), and S396A TyrH (short-dash line).

liquid helium temperatures, with *g* features between 10 and 2 consistent with an $S = {}^5/_2$ system (*13*). EPR spectroscopy was performed with each of the mutant enzymes to determine if there were any detectable perturbations in the iron environment. The EPR spectra of the S395A and S396A enzymes were indistinguishable from that of the wild-type enzyme (data not shown).

An alternative approach to probing the metal environment in TyrH is to utilize the charge-transfer complex formed upon binding of catecholamines to the Fe(III) enzyme (*14*, *15*). The presence of bound catecholamines interacting with the active site iron results in a broad absorbance band around 700 nm (*15*, *16*). Minor perturbations in the ligand environment can lead to shifts in this ligand to metal charge-transfer band (*17*). The addition of dopamine to the wild-type or mutant proteins resulted in indistinguishable absorbance spectra with maxima at 700 nm (data not shown).

Steady-State Kinetic Analyses of Mutant Enzymes. The abilities of the S395A and S396A proteins to catalyze DOPA formation were assessed. The specific activity of S396A TyrH was 1.97 ± 0.03 μmol of DOPA min^{-1} (mg of protein)$^{-1}$, similar to the value for the wild-type enzyme of 2.84 ± 0.02. The S395A protein exhibited an approximately 70-fold decrease in specific activity, with a value of 0.0382 ± 0.003. In contrast, the more conservative mutation of Ser395 to threonine, which should still form the proposed hydrogen bond to His331, resulted in an only 3-fold decrease in the specific activity for DOPA formation (0.726 ± 0.005).

Because of the very low rate of DOPA formation catalyzed by S395A TyrH, the steady-state kinetic parameters of the mutant enzymes were determined by measuring rates of tetrahydropterin oxidation. For both mutant proteins, the K_M values for tyrosine, BH$_4$, and 6-MPH$_4$ and the V_{max} values for tetrahydropterin oxidation are nearly identical to the wild-type values (Table 1). In contrast, there is a large decrease in the efficiency with which the tetrahydropterin is utilized to form DOPA by the S395A enzyme, in that the amount of DOPA formed is only 2% of the amount of tetrahydropterin oxidized. Thus, the decrease in the specific activity of S395A TyrH is due to the vast majority of the tetrahydropterin being consumed without concomitant hydroxylation of tyrosine. In contrast, mutation of Ser396 does not significantly affect any of the kinetic parameters, including the relative stoichiometry of tetrahydropterin oxidation and DOPA formation.

Table 1: Steady-State Kinetic Parameters of Serine Mutants of Tyrosine Hydroxylase[a]

enzyme	K_{tyr} (μM)	K_{6-MPH4} (μM)	K_{BH4} (μM)	V_{max} (min^{-1})	specific activity[b] (μmol of DOPA min^{-1} mg^{-1})	DOPA/dihydropterin
wild-type TyrH	29.1 ± 4.2	68.5 ± 2.3	55.6 ± 1.2	111 ± 4.3	2.84 ± 0.020	0.94 ± 0.05
S395A TyrH	32.2 ± 2.3	78.6 ± 2.4	59.2 ± 2.7	112 ± 3.7	0.038 ± 0.003	0.020 ± 0.003
S396A TyrH	24.2 ± 2.7	61.1 ± 2.4	46.0 ± 1.4	137 ± 4.5	1.97 ± 0.030	0.89 ± 0.07

[a] Kinetic parameters were determined by measuring the rate of tetrahydropterin oxidation by TyrH in the presence of 100 μg/mL catalase, 10 μM ferrous ammonium sulfate, 200 μM NADH, 0.1 unit/mL dihydropteridine reductase, and 50 mM HEPES/NaOH at pH 7.0 and 25 °C. [b] The assay measured the level of DOPA formation from tyrosine with 50 mM HEPES/NaOH, 100 μg/mL catalase, 10 μM ferrous ammonium sulfate, 250 μM tyrosine, and 300 μM 6-MPH$_4$ at pH 7.0 and 32 °C.

Identification of the Pterin Products of S395A TyrH. The assay used to determine the rate of tetrahydropterin oxidation is a coupled assay, monitoring the decrease in the absorbance at 340 nm when the quinonoid dihydropterin that is produced is reduced back to the tetrahydropterin by pyridine nucleotide-dependent dihydropteridine reductase. This assay can be used for the wild-type enzyme because the hydroxypterin product readily dehydrates to the quinonoid dihydropterin. Because the assay actually measures the rate of formation of the quinonoid dihydropterin, it will not distinguish enzyme-catalyzed formation of the hydroxypterin and its subsequent dehydration to quinonoid dihydropterin from direct enzyme-catalyzed formation of quinonoid dihydropterin. This is not a concern with the wild-type enzyme when tyrosine is the substrate, since the stoichiometry shown in Scheme 1 is well-established. However, in the case of the S395A enzyme, the inability to distinguish the two pterin products means that the excess tetrahydropterin oxidation could be producing either quinonoid dihydropterin, hydroxypterin, or both.

HPLC was used to identify the pterin products of the reaction catalyzed by the S395A enzyme. Twenty seconds after the initiation of turnover with either the mutant or the wild-type enzyme, an aliquot of the reaction mixture was injected onto an HPLC column. Peaks were detected at both 246 and 300 nm. The identities of the individual peaks were determined by using a diode array detector to determine their spectra during the chromatography. With both enzymes, both the 4a-hydroxypterin and the quinonoid dihydropterin were formed. No other pterin products were detected (results not shown).

While this result establishes that the S395A enzyme can make the hydroxypterin, the rapid dehydration of this compound during the chromatography ruled out HPLC as a method for determining the stoichiometry of hydroxypterin formation. To determine how much of the tetrahydropterin is converted to the hydroxypterin by the mutant enzyme, we took advantage of the distinctive absorbance spectra of the 4a-hydroxypterin and the quinonoid dihydropterin. The largest difference is at 246 nm, where the 4a-hydroxypterin has an absorbance maximum. The changes in the pterin spectra when wild-type TyrH and each of the mutant enzymes catalyze the consumption of 100 μM 6-methyltetrahydropterin were determined. Relatively high concentrations of each enzyme (10 μM) were used to minimize the amount of nonenzymatic autoxidation. In addition, the reactions were carried out at pH 8 to decrease the rate of dehydration of the hydroxypterin to the quinonoid dihydropterin (*18*). Figure 3A shows the results of such an experiment with the S395A protein. There is the clear formation of a transient species with an absorbance maximum at 246 nm, as expected if the 4a-hydroxypterin is formed in significant amounts and then dehydrates to the quinonoid dihydropterin.

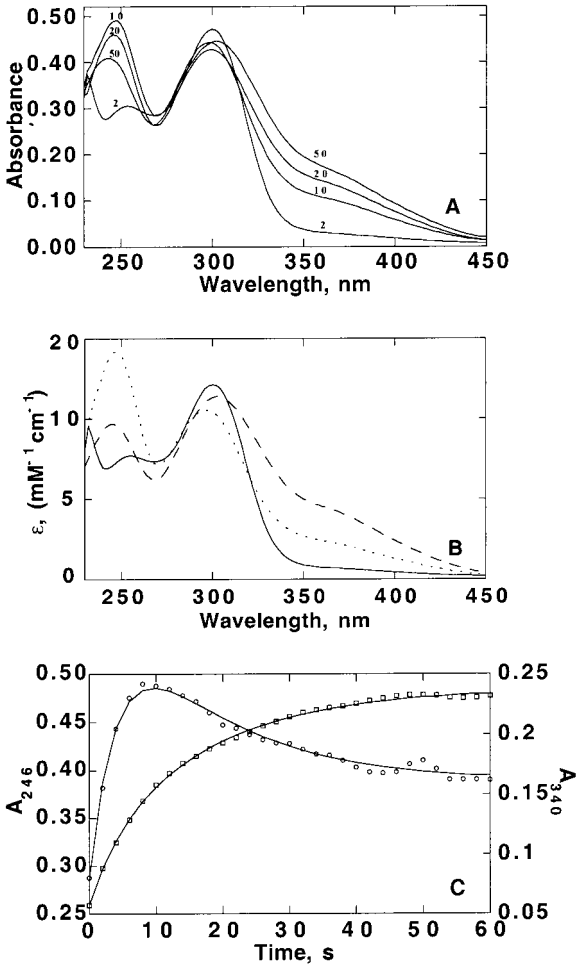

FIGURE 3: UV−visible spectra of 4a-hydroxypterin formation by S395A TyrH. (A) Spectral changes during the consumption of 100 μM 6-MPH$_4$ by 10 μM S395A TyrH, with 150 μM tyrosine, 10 μM ferrous ammonium sulfate, and 50 mM HEPES at pH 8.0 and 25 °C. The spectra that are shown were taken at the indicated times (in seconds) after initiation of the reaction. (B) Calculated spectra of individual pterin species. Spectra of intermediates during the reaction described for panel A were calculated by fitting all of the spectra taken for 200 s at 2 s intervals to the model of Scheme 2. The spectra that are shown are for 6-methyltetrahydropterin (solid line), 4a-hydroxypterin (dotted line), and quinonoid dihydropterin (dashed line). (C) Comparison between experimental absorbance changes vs time at 246 and 340 nm and those calculated from the fit to Scheme 2. The actual absorbances at 246 nm are given by the circles and those at 340 nm by the squares. The lines are the calculated absorbances.

The spectral changes were analyzed with the global analysis program SPECFIT using the model shown in

Table 2: Rate Constants for Pterin Product Formation by S395A, S396A, and Wild-Type Tyrosine Hydroxylase[a]

enzyme	k_1 (s^{-1})	k_2 (s^{-1})	k_3 (s^{-1})	k_4 (s^{-1})	% 4a-hydroxypterin formed
wild-type TyrH	0.60 ± 0.02	0.054 ± 0.002	0.013 ± 0.0001	0.0047 ± 0.002	97.8 ± 1.2
S396A TyrH	0.36 ± 0.02	0.054 ± 0.002	0.018 ± 0.0008	0.0085 ± 0.0009	95.2 ± 0.80
S395A TyrH	0.22 ± 0.04	0.061 ± 0.003	0.011 ± 0.0009	0.0045 ± 0.0009	95.3 ± 1.6

[a] The amount of 4a-hydroxypterin formed was determined from the spectral changes during the consumption of 100 μM 6-MPH_4 by 10 μM TyrH in 50 mM HEPES, 150 μM tyrosine, and 10 μM ferrous ammonium sulfate at pH 8.0 and 25 °C. Spectra were taken from 235 to 500 nm at 2 s intervals for a total of 200 s. The concentrations of the individual pterins and the rates of their formation were determined by fitting the spectra globally to the mechanism of Scheme 2.

Scheme 2. For a given model, SPECFIT will utilize the complete spectral changes over time to calculate spectra for the individual species defined in the model and the rate constants for the formation of each species. In the model shown in Scheme 2, 6-MPH_4 is oxidized either enzymatically to the 4a-hydroxypterin with the rate k_1 or directly to the quinonoid dihydropterin with the rate k_3. The 4a-hydroxypterin then dehydrates in solution to quinonoid dihydropterin with the rate constant k_2. Finally, the quinonoid dihydropterin tautomerizes to form the 7,8-dihydropterin with the rate constant k_4. The relatively low rate for the nonenzymatic oxidation of 6-methyltetrahydropterin to quinonoid dihydropterin was not included in the model. Figure 3B shows the spectra for the dihydropterin and the quinonoid dihydropterin calculated from the data obtained with the S395A protein. The spectra agree reasonably well with previously reported spectra for these species (*19*). Figure 3C shows a comparison of the calculated and observed spectral changes at 246 nm, where the absorbance of the hydroxypterin is greatest, and at 340 nm, where the absorbance of the quinonoid dihydropterin makes the greatest contribution. The rates obtained by fitting the spectral changes for the wild-type and mutant proteins to the mechanism of Scheme 2 are summarized in Table 2. The relative amounts of 4a-hydroxypterin and quinonoid dihydropterin formed enzymatically can be calculated from the values of k_1 and k_3. For all three enzymes, there is essentially stoichiometric formation of the hydroxypterin. In addition, the rates of formation of the 4a-hydroxypterin are similar for all three enzymes.

DISCUSSION

The conserved active site residues shown in Figure 1 were identified by analyses of the available sequences of all three pterin-dependent hydroxylases in combination with the three-dimensional structure of TyrH. To date, site-directed mutagenesis of several of these residues has provided information regarding their catalytic roles. Replacement of His331 or His336 with alanine results in a loss of catalytic activity and iron binding, consistent with their roles as metal ligands (*13*). Mutation of Arg316 or Asp328 significantly increases the K_M value for tyrosine, implicating these residues in binding of the amino acid substrate (*6*). Mutation of Glu332 or Phe300 results in an increase in the K_M value for 6-MPH_4 (*6*), consistent with the conclusions from structural data that these residues are important in maintaining the correct orientation of the pterin for catalysis (*20*). Mutation of Phe309 or Glu326 has little effect on K_M values, but decreases the V_{max} value for DOPA production and results in an excess of tetrahydropterin consumption over DOPA production, consistent with a disruption of the overall active site structure (*6*, *7*). Mutation of Tyr371 to phenylalanine has no effect on the ability of the enzyme to catalyze the hydroxylation of tyrosine to DOPA, although it does decrease the K_M value for phenylalanine by an order of magnitude, consistent with the lack of a catalytic role for this residue (*5*). Ser395 and Ser396 are two remaining active site residues conserved among the family of pterin-dependent hydroxylases. The hydroxyl oxygen of Ser395 is located 2.78 Å from the imidazole N-1 of the iron ligand His331, an appropriate distance for a hydrogen bond. Ser396 is also located within the active site; however, a role for Ser396 is not as apparent from the three-dimensional structure. The goal of this study was to determine the roles of these conserved residues in catalysis.

The structural characterizations of the mutant proteins suggest that the replacement of either serine with alanine does not result in any gross changes in overall structure. In addition, the coordination of the metal is unchanged, given the lack of an effect on the spectral properties associated with the metal and on the ability of both S395A and S396A TyrH to bind a stoichiometric amount of iron. On the basis of these results, neither serine residue is critical for the structural integrity of TyrH.

In terms of the catalytic roles of these two residues, the results of mutating Ser396 to alanine are easiest to interpret. Ser396 simply does not play an essential role in catalysis. The K_M values for tyrosine, $6MPH_4$, and BH_4 are unchanged by the mutation, while the V_{max} value is similar to the wild-type value. In addition, tetrahydropterin consumption is still tightly coupled to tyrosine hydroxylation by this enzyme.

In contrast, mutation of Ser395 has significant effects on the ability of tyrosine hydroxylase to catalyze hydroxylation of tyrosine. There are no alterations in the K_M values for 6-MPH_4, BH_4, or tyrosine, suggesting that Ser395 does not play a direct role in the binding of any of these substrates.[2] However, the ability of the enzyme to hydroxylate tyrosine is severely compromised by the loss of the serine hydroxyl. The relatively high activity of the S395T enzyme confirms the importance of the hydroxyl. The 2 order of magnitude decrease in the ability to form DOPA is not due to an inability to catalyze the reaction of the enzyme with oxygen. The kinetics of tetrahydropterin oxidation establish that the early steps in catalysis are not significantly affected by the

[2] Recently, Teigen et al. (*21*) proposed a model for the binding of both phenylalanine and tetrahydrobiopterin in the active site of phenylalanine hydroxylase. In this model, the amino group of the substrate phenylalanine interacts with the side chains of Ser349, the residue homologous to Ser395 of TyrH, and Arg270, the residue homologous to Arg316 of TyrH. The lack of a change in the K_M value for tyrosine in S395A TyrH does not support this proposal. This result can be compared with the 4 order of magnitude decrease in the affinity of TyrH for tyrosine upon mutation of Arg316 to lysine (*6*).

Scheme 3

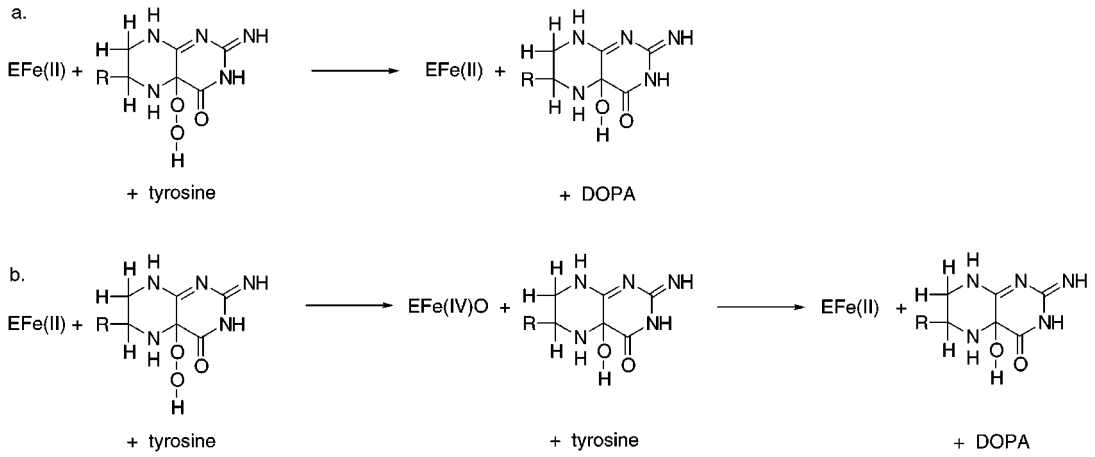

mutation. It is only steps after the formation of the 4a-hydroxypterin which are drastically affected.

The identity of the hydroxylating intermediate remains unknown for the pterin-dependent hydroxylases. A 4a-peroxypterin has been proposed as an intermediate in the reactions catalyzed by these enzymes on the basis of model studies and on the basis of kinetic isotope effects with TyrH (*11*, *22*).[3] Such a 4a-peroxypterin would be similar to the 4a-peroxyflavin proposed as the hydroxylating intermediate for flavin phenol hydroxylases (*24*). If the peroxypterin is the hydroxylating intermediate, cleavage of the oxygen−oxygen bond would be concerted with the hydroxylation of the amino acid substrate and result in the direct formation of the 4a-hydroxypterin (Scheme 3a), as is the case with the flavoproteins (*24*, *25*). In contrast, studies of the reaction of phenylalanine hydroxylase with tyrosine as the substrate suggest that cleavage of the oxygen−oxygen bond in the peroxypterin results in the transfer of one oxygen atom to the iron which forms a high-valence ferryl oxo intermediate and the 4a-hydroxypterin (Scheme 3b) (*26*, *27*). This ferryl oxo intermediate would then hydroxylate the aromatic ring of the amino acid in a subsequent step. The stoichiometric formation of 4a-hydroxypterin by a TyrH which is severely compromised in its ability to catalyze amino acid hydroxylation establishes that oxygen−oxygen bond cleavage can occur in the absence of oxygen transfer to the amino acid. This result clearly rules out concerted oxygen−oxygen bond cleavage and carbon−oxygen bond formation. It is most consistent with the hydroxylating intermediate being a ferryl oxo species formed by cleavage of the oxygen−oxygen bond of a peroxypterin rather than the peroxypterin itself. Very recently, Lange et al. (*28*) have described a nonenzymatic system in which cleavage of the oxygen−oxygen bond of a peroxide similarly generates a ferryl oxo species capable of aromatic hydroxylation.

Replacement of Glu332 of TyrH with alanine results in a 2 order of magnitude decrease in the V_{max} value for DOPA formation and only a 3-fold decrease in the V_{max} value for tetrahydropterin oxidation (*6*). The effects of that mutation resemble those described here for the S395A enzyme, in that the oxidation of tetrahydropterin has become decoupled from hydroxylation of the amino acid. The increase in the K_M value for tetrahydropterin in the E332A enzyme suggested that this residue plays a role in pterin binding, a conclusion confirmed by the structure of the enzyme−dihydrobiopterin structure (*20*). However, in contrast to the results seen upon mutation of Ser395, the E332A enzyme does not catalyze the stoichiometric formation of the hydroxypterin (*6*). The effects of both mutations can be accommodated by the mechanism shown in Scheme 4. Here, oxygen initially reacts with the tetrahydropterin to form a peroxypterin. No explicit role for the metal is given for this step, consistent with the observation by Chen and Frey that the phenylalanine hydroxylase from *Chromobacterium violaceum* can catalyze tetrahydropterin oxidation in the absence of bound metal (*29*). The peroxypterin would then react with the iron in a reaction reminiscent of the cytochrome P450 hydroxylases (*30*) to form the ferryl oxo species, the actual hydroxylating intermediate. The subsequent hydroxylation of the amino acid to complete the reaction is shown to occur via a cationic intermediate, consistent with the results of Hillas and Fitzpatrick (*31*). In the mechanism of Scheme 4, the lesion in the E332A enzyme would be in the reaction of the peroxypterin with the iron to form the hydroxylating intermediate due to the altered pterin binding resulting from the mutation. In the case of the S395A enzyme, the reaction of oxygen and the tetrahydropterin to generate the peroxypterin still occurs, since binding of the pterin is unaffected by the mutation. However, the loss of the hydrogen bond from the imidazole of His331 to the hydroxyl group of Ser395 results in the destabilization of the ferryl intermediate once it has formed. This results in the breakdown of this species before it can react with the amino acid.

The structure of the catalytic domain of TyrH shows the iron atom in a square pyramidal arrangement. His336, Glu376, and two water molecules are the equatorial ligands, and His331 is the axial ligand (*4*). In contrast, the structure of the homologous catalytic domain of PheH, which was determined at a slightly higher resolution, shows an octahedral iron site in which an additional water molecule provides the second axial ligand (*32*). Mössbauer and X-ray absorbance spectroscopic analyses of both the catalytic domain of TyrH and the intact enzyme are consistent with a

[3] An alternative possibility for the hydroxylating intermediate is a peroxypterin in which the distal peroxo oxygen is a ligand to the iron atom (*23*). The predictions of the timing of cleavage of the oxygen−oxygen bond of such a species are the same as for the peroxypterin itself.

Scheme 4

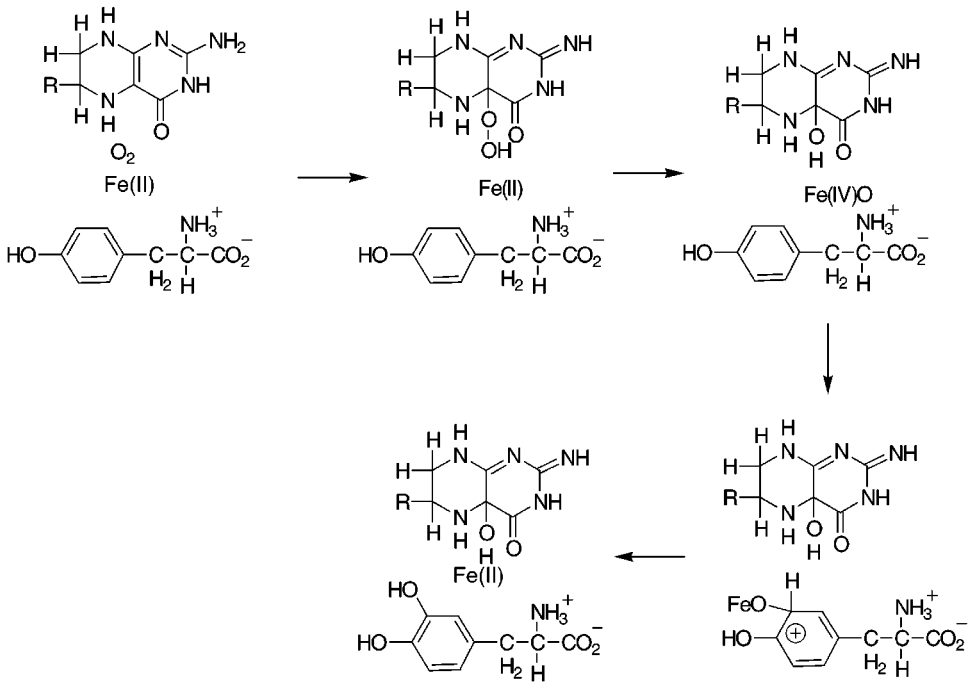

six-coordinate iron site which can be converted to a pentacoordinate site by dehydration, suggesting that the axial water molecule in TyrH is relatively labile (*33*). As noted above, the data presented here provide strong support for a ferryl oxo species as the hydroxylating intermediate in TyrH. The coordination position on the iron occupied by the labile axial water is the most likely site for oxygen to bind to the iron. Indeed, circular dichroic and magnetic circular dichroic spectral analyses of PheH show that the iron in that enzyme becomes pentacoordinate once both phenylalanine and pterin have bound, consistent with loss of the axial water to form an open position for oxygen (*34*). Disruption of a hydrogen bond between Ser395 and His331, the axial ligand distal to this site, would be expected to affect the interaction between oxygen and the iron. In myoglobin, there is a similar hydrogen bond between the hydroxyl of conserved Ser92 and the imidazole of the proximal His93. The effects of mutating this serine to alanine have been described for both human and pig myoglobin (*35*, *36*). Structural, spectral, and kinetic analyses established that the effects of the mutation are quite subtle. There are small changes in the orientation of the imidazole plane relative to the heme and an increase in the strength of the bond between the iron and N^{δ} of His93. The properties of the S395A mutant of TyrH are consistent with a similar small alteration in the electronic environment of the iron without significant changes in the overall active site structure. These changes are still sufficient to alter the stability of the hydroxylating intermediate.

The results described here show that mutation of Ser395 results in severe impairment of the ability of TyrH to hydroxylate tyrosine. This result is fully consistent with the existence of a critical hydrogen bond between Ser395 and the iron ligand His331. In addition, the ability of the mutant enzyme to catalyze formation of the hydroxypterin without the subsequent hydroxylation of tyrosine supports a ferryl oxo species rather than a peroxypterin as the hydroxylating intermediate. Finally, the results show that Ser396, although conserved within the family of pterin-dependent hydroxylase enzymes, is not an essential residue.

ACKNOWLEDGMENT

We thank Ellen Provin and Natalie Unruh of the Gene Technology Laboratory of the Biology Department of Teas A&M University for oligonucleotide synthesis and for DNA sequencing.

REFERENCES

1. Fitzpatrick, P. F. (1999) *Annu. Rev. Biochem. 68*, 355−381.
2. Hufton, S. E., Jennings, I. G., and Cotton, R. G. H. (1995) *Biochem. J. 311*, 353−366.
3. Kaufman, S., and Fisher, D. B. (1974) in *Molecular Mechanisms of Oxygen Activation* (Hayaishi, O., Ed.) pp 285−369, Academic Press, New York.
4. Goodwill, K. E., Sabatier, C., Marks, C., Raag, R., Fitzpatrick, P. F., and Stevens, R. C. (1997) *Nat. Struct. Biol. 4*, 578−585.
5. Daubner, S. C., and Fitzpatrick, P. F. (1998) *Biochemistry 37*, 16440−16444.
6. Daubner, S. C., and Fitzpatrick, P. F. (1999) *Biochemistry 38*, 4448−4454.
7. Ellis, H. R., Daubner, S. C., McCulloch, R. I., and Fitzpatrick, P. F. (1999) *Biochemistry 38*, 10909−10914.
8. Daubner, S. C., Hillas, P. J., and Fitzpatrick, P. F. (1997) *Biochemistry 36*, 11574−11582.
9. Daubner, S. C., Lauriano, C., Haycock, J. W., and Fitzpatrick, P. F. (1992) *J. Biol. Chem. 267*, 12639−12646.
10. Ramsey, A. J., Hillas, P. J., and Fitzpatrick, P. F. (1996) *J. Biol. Chem. 271*, 24395−24400.
11. Dix, T. A., and Benkovic, S. J. (1985) *Biochemistry 24*, 5839−5846.
12. Gampp, H., Maeder, M., Meyer, C. J., and Zuberbühler, A. D. (1985) *Talanta 32*, 95−101.
13. Ramsey, A. J., Daubner, S. C., Ehrlich, J. I., and Fitzpatrick, P. F. (1995) *Protein Sci. 4*, 2082−2086.
14. Andersson, K. K., Cox, D. D., Que, L., Jr., Flatmark, T., and Haavik, J. (1988) *J. Biol. Chem. 263*, 18621−18626.
15. Andersson, K. K., Vassort, C., Brennan, B. A., Que, L., Jr., Haavik, J., Flatmark, T., Gros, F., and Thibault, J. (1992) *Biochem. J. 284*, 687−695.

16. Haavik, J., Andersson, K. K., Petersson, L., and Flatmark, T. (1988) *Biochim. Biophys. Acta 953*, 142−156.
17. Cox, D. D., Benkovic, S. J., Bloom, L. M., Bradley, F. C., Nelson, M. J., Que, L., Jr., and Wallick, D. E. (1988) *J. Am. Chem. Soc. 110*, 2026−2032.
18. Bailey, S. W., Rebrin, I., Boerth, S. R., and Ayling, J. E. (1995) *J. Am. Chem. Soc. 117*, 10203−10211.
19. Lazarus, R. A., Dietrich, R. F., Wallick, D. E., and Benkovic, S. J. (1981) *Biochemistry 20*, 6834−6841.
20. Goodwill, K. E., Sabatier, C., and Stevens, R. C. (1998) *Biochemistry 37*, 13437−13445.
21. Teigen, K., Frøystein, N. Å., and Martinez, A. (1999) *J. Mol. Biol. 294*, 807−823.
22. Francisco, W. A., Tian, G., Fitzpatrick, P. F., and Klinman, J. P. (1998) *J. Am. Chem. Soc. 120*, 4057−4062.
23. Dix, T. A., Bollag, G., Domanico, P. L., and Benkovic, S. J. (1985) *Biochemistry 24*, 2955−2958.
24. Massey, V. (1994) *J. Biol. Chem. 269*, 22459−22462.
25. Entsch, B., Ballou, D. P., and Massey, V. (1976) *J. Biol. Chem. 251*, 2550−2563.
26. Davis, M. D., and Kaufman, S. (1989) *J. Biol. Chem. 264*, 8585−8596.
27. Davis, M. D., and Kaufman, S. (1988) *J. Biol. Chem. 263*, 17312−17316.
28. Lange, S. J., Miyake, H., and Que, L., Jr. (1999) *J. Am. Chem. Soc. 121*, 6330−6331.
29. Chen, D., and Frey, P. (1998) *J. Biol. Chem. 273*, 25594−25601.
30. Sono, M., Roach, M. P., Coulter, E. D., and Dawson, J. H. (1996) *Chem. Rev. 96*, 2841−2888.
31. Hillas, P. J., and Fitzpatrick, P. F. (1996) *Biochemistry 35*, 6969−6975.
32. Erlandsen, H., Fusetti, F., Martinez, A., Hough, E., Flatmark, T., and Stevens, R. C. (1997) *Nat. Struct. Biol. 4*, 995−1000.
33. Schunemann, V., Meier, C., Meyer-Klaucke, W., Winkler, H., Trautwein, A. X., Kappskog, P. M., Toska, K., and Haavik, J. (1999) *J. Inorg. Biochem. 4*, 223−231.
34. Kemsley, J. N., Mitic, N., Zaleski, K. L., Caradonna, J. P., and Solomon, E. I. (1999) *J. Am. Chem. Soc. 121*, 1528−1536.
35. Smerdon, S., Krzywda, S., Wilkinson, A., Brantley, R., Jr., Carver, T., Hargrove, M., and Olson, J. (1993) *Biochemistry 32*, 5132−5138.
36. Shiro, Y., Iizuka, T., Marubayashi, K., Ogura, T., Kitagawa, T., Balasubramanian, S., and Boxer, S. (1994) *Biochemistry 33*, 14986−14992.

BI9928546